

Spatial heterogeneity of Chl and CO₂ fluxes

F. S. Pacheco et al.

River inflow and retention time affecting spatial heterogeneity of chlorophyll and water–air CO₂ fluxes in a tropical hydropower reservoir

F. S. Pacheco¹, M. C. S. Soares², A. T. Assireu³, M. P. Curtarelli⁴, F. Roland², G. Abril⁵, J. L. Stech⁴, P. C. Alvalá¹, and J. P. Ometto¹

¹Earth System Science Center, National Institute for Space Research, São José dos Campos, 12227-010, São Paulo, Brazil

²Laboratory of Aquatic Ecology, Federal University of Juiz de Fora, Juiz de Fora, 36036-900, Minas Gerais, Brazil

³Institute of Natural Resources, Federal University of Itajubá, Itajubá, 37500-903, Minas Gerais, Brazil

⁴Remote Sense Division, National Institute for Space Research, São José dos Campos, 12227-010, São Paulo, Brazil

⁵Laboratoire Environnements et Paléoenvironnements Océaniques et Continentaux (EPOC), CNRS, Université Bordeaux 1, Avenue des Facultés, 33405 Talence, France

Title Page

Abstract

Introduction

Conclusions

References

Tables

Figures



Back

Close

Full Screen / Esc

Printer-friendly Version

Interactive Discussion



Received: 15 April 2014 – Accepted: 6 May 2014 – Published: 11 June 2014

Correspondence to: F. S. Pacheco (felipe.pacheco@inpe.br)

Published by Copernicus Publications on behalf of the European Geosciences Union.

BGD

11, 8531–8568, 2014

Spatial heterogeneity of Chl and CO₂ fluxes

F. S. Pacheco et al.

Title Page

Abstract

Introduction

Conclusions

References

Tables

Figures



Back

Close

Full Screen / Esc

Printer-friendly Version

Interactive Discussion



Abstract

Much research has been devoted to understanding the complexity of biogeochemical and physical processes responsible for the greenhouse gas (GHG) emissions from hydropower reservoirs. Spatial complexity and heterogeneity of GHG emission may be observed in these systems because it is dependent on flooded biomass, river inflow, primary production and dam operation. In this study, we investigate the relationships between water–air CO₂ fluxes and phytoplanktonic biomass in Funil Reservoir, an old and stratified tropical reservoir, where intense phytoplankton blooms and low partial pressure of CO₂ ($p\text{CO}_2$) are observed. Our results showed that Funil Reservoir seasonal and spatial variability of chlorophyll concentration (Chl) and $p\text{CO}_2$ is more related to changes in river inflow over the year than environmental factor such as air temperature and solar radiation. Field data and hydrodynamic simulations reveal that the river inflow contributes to increased heterogeneity in dry season due to the variation of reservoir retention time and river temperature. Contradictory conclusion can be drawn if temporal data collected only near the dam is considered instead of spatial data to represent CO₂ fluxes in whole reservoir. The average CO₂ fluxes was -17.6 and $22.1 \text{ mmol m}^{-2} \text{ d}^{-2}$ considering data collected near the dam and spatial data, respectively, in periods of low retention time. In this case, the lack of spatial information can change completely the role of Funil Reservoir regarding GHG emissions. Our results support the idea that Funil Reservoir is a dynamic system where the hydrodynamics represented by changes in river inflow and retention time is potentially more important force driving both Chl and $p\text{CO}_2$ spatial variability than in-system ecological factors.

1 Introduction

Over the last two decades, hydropower reservoirs have been identified as potentially important sources of greenhouse gas (GHG) emissions (St Louis et al., 2000; Rosa et al., 2004; Demarty et al., 2011). In tropical region, high temperatures and the flood-

BGD

11, 8531–8568, 2014

Spatial heterogeneity of Chl and CO₂ fluxes

F. S. Pacheco et al.

Title Page

Abstract

Introduction

Conclusions

References

Tables

Figures

◀

▶

◀

▶

Back

Close

Full Screen / Esc

Printer-friendly Version

Interactive Discussion



**Spatial heterogeneity
of Chl and CO₂ fluxes**

F. S. Pacheco et al.

[Title Page](#)[Abstract](#)[Introduction](#)[Conclusions](#)[References](#)[Tables](#)[Figures](#)[I ◀](#)[▶ I](#)[◀](#)[▶](#)[Back](#)[Close](#)[Full Screen / Esc](#)[Printer-friendly Version](#)[Interactive Discussion](#)

ing of large amounts of biomass, including primary forest, result to intense GHG emission (Abril et al., 2005; Fearnside and Pueyo, 2012). However, emissions are larger in tropical Amazonian (Abril et al., 2013) than in tropical Cerrado reservoirs (Ometto et al., 2011) and in younger than in older reservoirs (Barros et al., 2011). Large hydroelectric reservoirs, especially those created by impounding rivers, are morphometrically complex and spatially heterogeneous (Roland et al., 2010; Teodoru et al., 2011; Zhao et al., 2013). Different regions in terms of CO₂ may be observed in these systems because it is dependent on flooded biomass, river input of organic matter, primary production and dam operation regime. Furthermore, both heterotrophic and autotrophic activity influences CO₂ concentration along reservoirs and the role of these activities has been reported in subtropical (Di Siervi et al., 1995), tropical (Roland et al., 2010; Kemenes et al., 2011) and temperate areas (Richardot et al., 2000; Lauster et al., 2006; Finlay et al., 2009; Halbedel and Koschorreck, 2013).

As the sedimentation and light availability increase along the reservoir, biomass of primary producers may increase. The phytoplankton is distributed in patches along the reservoir due to differences in habitat conditions linked to nutrient distribution, light availability and stratification (Serra et al., 2007). Also, hydrodynamics factors as retention time and river inflow showed to influence the phytoplankton communities and growth (Vidal et al., 2012; Soares et al., 2008). Intense phytoplankton primary production has been identified as the main regulator of carbon (C) budget in temperate eutrophic lakes (Finlay et al., 2010; Pacheco et al., 2014), however the impact on tropical hydropower reservoir is still unclear.

River inflows may affect biogeochemical patterns in river valley reservoirs (Kennedy, 1999). Difference on density of the incoming stream and lake water, stream and lake hydraulics, strength of stratification and mixing are features that control how the river water will flow when it reaches the reservoir (Fischer and Smith, 1983; Fischer et al., 1979). As result of density differences between river and lake water, the river enters in the lake and can flow large distances as a gravity-driven density current (Ford, 1990; Martin and McCutcheon, 1998). The interaction of large nutrient load injected by river

and the dynamic of river inflow can determine the spatial heterogeneity in phytoplankton distribution (Vidal et al., 2012). Consequently, river inflow may affect primary production along river/dam axis in hydropower reservoirs strongly influenced by river.

In this study, we investigate the relationships between phytoplanktonic biomass and water–air CO₂ fluxes in an old and stratified tropical reservoir (Funil, state of RJ, Brazil), where intense phytoplankton blooms and low pCO₂ are observed in the water. We combine fieldwork and modeling to analyze the respective impact of meteorological and hydrological factors on the spatial and temporal dynamics of phytoplankton and the intensity of CO₂ fluxes. We show the effect of the river inflow in the heterogeneity of pCO₂ and Chl in Funil reservoir. We also compare temporal data of pCO₂ collected near the dam with a high dense spatial data. Our hypothesis were that (1) seasonal and spatial variability of pCO₂ and Chl in Funil Reservoir is more related to river inflow and retention time than external environmental factor such as air temperature and solar radiation and, (2) very different conclusion can be drawn regarding carbon cycle in reservoir if spatial heterogeneity is not adequately considered.

2 Materials and methods

2.1 Study site

Funil Reservoir is an old impoundment constructed at the end of the 1960s and is located on Paraíba do Sul River, in a southern city (Resende) of the Rio de Janeiro State, Brazil (22°30' S, 44°45' W, Fig. 1). It is 440 m a.s.l., with wet-warm summers and dry-cold winters (Cwa, Köppen system). The main purpose of Funil Reservoir is energy production, but the reservoir is also used for irrigation and recreation. It has a surface area of 40 km², mean and maximum depth of 22 and 74 m, respectively, and total volume of 890 × 10⁶ m³. The maximum and minimum reservoir water level occurs in the end of rainy season (April) and dry season (October), respectively. From October 2011

BGD

11, 8531–8568, 2014

Spatial heterogeneity of Chl and CO₂ fluxes

F. S. Pacheco et al.

Title Page

Abstract

Introduction

Conclusions

References

Tables

Figures

◀

▶

◀

▶

Back

Close

Full Screen / Esc

Printer-friendly Version

Interactive Discussion



to September 2012, the difference between minimum and maximum water level was 15.6 m.

Funil Reservoir has a catchment area of 12 800 km² that has a high demographic density. The river inflow is not restrictedly linked to the rainfall in the watershed because it also depends on the water supply-demand and operation of dams constructed upstream. There are around 2 million people living inside the catchment area and 39 cities depending on the Paraíba do Sul River for water supply. These cities comprises 2 % of Brazil's gross domestic product (GDP) (IBGE, 2010). In this area, 46 % of sewage is untreated (AGEVAP, 2011) and the Paraíba do Sul River receives a large portion of the sewage from one of the main Brazilian industrial areas crossing part of the São Paulo State. Consequently, the river has a large influence on reservoir's water quality that has experienced tragic eutrophication in recent decades, resulting in frequent and intense cyanobacterial blooms (Klapper, 1998; Branco et al., 2002; Rocha et al., 2002). In general, Funil Reservoir is a turbid, eutrophic system, with high phytoplankton (cyanobacteria) biomass (Soares et al., 2012; Rangel et al., 2012).

2.2 Field sampling

Spatial data – the water samples for Chl and *p*CO₂ were taken between 09:00 LT and 12:00 LT on 1 March 2012 (end of rainy season, high water level) and 20 September 2012 (end of dry season, low water level). Samples were taken at the surface (0.3 m) at 42 stations in Funil Reservoir (28 located along the main body of the reservoir, Fig. 1) in the same day to limit the effect of diurnal variation on the results.

We measured the Chl using a compact version of PHYTO-PAM (Heinz Walz GmbH, PHYTO-ED, Effelrich, Germany). Functionally the PHYTO-ED displays the same features as the standard but has distinct advantages for fieldwork. In the PHYTO-PAM Phytoplankton Analyzer μ sec measuring light pulses are generated by an array of light-emitting diodes (LED) featuring 4 different colors: blue (470 nm), green (520 nm), light red (645 nm) and dark red (665 nm). The differently colored measuring light pulses are applied alternatingly at a high frequency, such that quasi-simultaneous information on

BGD

11, 8531–8568, 2014

Spatial heterogeneity of Chl and CO₂ fluxes

F. S. Pacheco et al.

Title Page

Abstract

Introduction

Conclusions

References

Tables

Figures

◀

▶

◀

▶

Back

Close

Full Screen / Esc

Printer-friendly Version

Interactive Discussion



Chl fluorescence excited at the 4 different wavelengths is obtained. Following proper calibration, this feature allows to differentiate between the contributions of the main types of phytoplankton (green, blue, brown algae) with different pigment systems. In addition, Chl content of the various types can be estimated.

5 The $p\text{CO}_2$ data were determine using water–air equilibration method. In a marble-type equilibrator (Abril et al., 2014, 2006), water pumped directly from the lake flows from the top to the bottom (0.8 liters per min), while a constant volume of air (0.4 liters per min) flows from the bottom to the top. The large gas exchange surface area promoted by the contact with the marbles accelerates the $p\text{CO}_2$ water–air equilibrium.
10 The air pump conduct the air from the top of the equilibrator through a drying tube containing a desiccant (Drierite), then to an infrared gas analyzer (IRGA, LI-840, LICOR, Lincoln, Nebraska, USA), and then back to the bottom of the equilibrator (closed air circuit, Abril et al., 2006). For each station, the lake water and air were pumped through this system for two minutes before the $p\text{CO}_2$ from the IRGA stabilized to a constant value.
15

Color maps were created to represent spatial distribution of Chl and $p\text{CO}_2$ (Fig. 2). We used variogram analysis to describe spatial correlation among samples and to spatially interpolate using Kriging methods (Bailey and Gatrell, 1995). The empirical variograms were fitted to different mathematical models using Akaike's information criterion (AIC, Akaike, 1974) to evaluate the best fit. The best model variogram were used for interpolation by ordinary kriging. The root mean-square error (RMSE), calculated comparing observed and calculated values, was $90 \mu\text{atm}$ and $15 \mu\text{g L}^{-1}$ for $p\text{CO}_2$ and Chl, respectively. We used the software Spring (Câmara et al., 1996) version 5.1.8 to conduct the spatial analysis and to produce the in situ $p\text{CO}_2$ and Chl maps.
20

25 *Time series data* – wind speed and direction, solar radiation, pH, dissolved oxygen (DO), air temperature and temperature profiles (2 m, 5 m, 20 m and 40 m depth) were collected hourly at station S28 near the dam (Fig. 1) and transmitted by satellite in quasi-real time by the Integrated System for Environmental Monitoring (SIMA). The SIMA is a set of hardware and software developed for data acquisition and real-time

Spatial heterogeneity of Chl and CO_2 fluxes

F. S. Pacheco et al.

[Title Page](#)[Abstract](#)[Introduction](#)[Conclusions](#)[References](#)[Tables](#)[Figures](#)[◀](#)[▶](#)[◀](#)[▶](#)[Back](#)[Close](#)[Full Screen / Esc](#)[Printer-friendly Version](#)[Interactive Discussion](#)

monitoring of hydrological systems (Alcantara et al., 2013; Stevenson et al., 1993). The SIMA consists of an independent system formed by an anchored buoy containing data storage systems, sensors (air temperature, wind direction and intensity, pressure, incoming and reflected radiation and a thermistor chain), a solar panel, a battery and a transmission antenna. A sonde (YSI model 6600, Yellow Spring, Ohio, USA) was attached to the SIMA buoy to collect hourly surface data on temperature, conductivity, pH, and oxygen. This sonde was calibrated every 15 days according to the YSI Environmental Operations Manual (<http://www.ysi.com/ysi/support>).

We calculated the $p\text{CO}_2$ in the surface water over one year near the dam from measured pH and alkalinity. The calculations include dependence on temperature for dissociation constants of carbonic acid (Millero et al., 2002) and solubility of CO_2 . We used pH and temperature collected by SIMA between 25 October 2011 and 25 October 2012 and monthly data of alkalinity determined by the titration method (APHA, 2005) at station S28 (Fig. 1). Samples for total phosphorous (TP) and nitrogen (TN) were taken monthly. For TP, the samples was oxidized by persulfate and then analyzed as soluble reactive phosphorus. TN was determined as the sum of organic fraction measured by Kjeldahl method and the dissolved inorganic nutrients. Laboratory analysis for TP and NP was performed according to standard spectrophotometric techniques (Wetzel and Likens, 2010).

2.3 CO_2 flux calculation

The air-water flux of CO_2 ($\text{mmol m}^{-2} \text{d}^{-1}$) was calculated according to Eq. (1).

$$F(\text{CO}_2) = k\alpha\Delta p\text{CO}_2 \quad (1)$$

Where k is the gas transfer velocity of CO_2 (in cm h^{-1}), α is the solubility coefficient of CO_2 (in $\text{mol kg}^{-1} \text{atm}^{-1}$) as a function of water temperature (Weiss, 1974), and $\Delta p\text{CO}_2$ is the air-water gradient of $p\text{CO}_2$ (in μatm). The atmospheric $p\text{CO}_2$ measured in the rainy and dry season was $375 \mu\text{atm}$ and this atmospheric value was used for all flux

Spatial heterogeneity of Chl and CO_2 fluxes

F. S. Pacheco et al.

Title Page

Abstract

Introduction

Conclusions

References

Tables

Figures

◀

▶

◀

▶

Back

Close

Full Screen / Esc

Printer-friendly Version

Interactive Discussion



calculation. The gas transfer velocity k was calculated from the gas transfer velocity normalized to a Schmidt number of 600 that corresponds to CO_2 at 20°C (Eq. 2) (Jahne et al., 1987). Positive values of CO_2 fluxes denotes net gas flux from the lake to the atmosphere.

$$k = k_{600} \left(\frac{600}{Sc} \right)^{-0.5} \quad (2)$$

Where k_{600} is the normalized gas transfer velocity calculated according to the following equation (Cole and Caraco, 1998), Sc is the Schmidt number of a given gas at a given temperature (Wanninkhof, 1992).

$$k_{600} = 2.07 + 0.21U_{10}^{1.7} \quad (3)$$

Where U_{10} is wind speed at 10 m height. The wind speed was obtained from the SIMA da at 3 m height and was calculated for 10 m height (Smith, 1985).

In riverine zone, we considered the k_{600} as a function of wind and water current. The contribution of the water current to the gas transfer velocity was estimated using the water current (cm s^{-1}), depth (m) and the equations in Borges et al. (2004).

2.4 Temperature profile

Temperature profiles were collected using thermistor chain deployed at station S09 in rainy season and station S14 in dry season to determine the thermal structure at transition zone. Eleven thermistors (Hobo, U22 Water Temp Pro v2, Bourne, Massachusetts, USA) were placed every 0.5 m up to 4 m and every 1 m from 5 to 7 m. We also deployed a thermistor chain at riverine zone at station S05 with thermistors placed every 2 m. The thermistors were programmed to record temperature every 10 min. In the rainy season, the thermistor chain was deployed on 29 February 2012 at 18:30 LT and recovered after 40 h. In the dry season, the thermistor chain was deployed on 20 September 2012 at 11:30 LT and recovered after 25 h.

BGD

11, 8531–8568, 2014

Spatial heterogeneity of Chl and CO_2 fluxes

F. S. Pacheco et al.

Title Page

Abstract

Introduction

Conclusions

References

Tables

Figures

◀

▶

◀

▶

Back

Close

Full Screen / Esc

Printer-friendly Version

Interactive Discussion



In our analysis, temperature is considered as the factor controlling water density. The use of temperature is justified by the low conductivity and turbidity in the river. The values of turbidity measured in the field of 29 and 11 NTU in rainy and dry seasons, respectively, would have effected density < 5 % relative to that of temperature (Gippel, 1989).

2.5 Numerical Model description and setup

Numerical simulations of lake hydrodynamics were conducted with the Estuary and Lake Computer Model (ELCOM, Hodges et al., 2000), which solves the 3-D hydrostatic, Boussinesq, Reynolds-averaged Navier–Stokes and scalar transport equations, separating mixing of scalars and momentum from advection. The hydrodynamic algorithms that are implemented in ELCOM use an Euler–Lagrange approach for the advection of momentum adapted from the work of Casulli and Cheng, 1992, whereas the advection of scalars (i.e., tracers, conductivity and temperature) is based on the ULTIMATE QUICKEST method proposed by Leonard, 1991). The thermodynamics model considers the penetrative (i.e., shortwave radiation) and non-penetrative components (i.e., longwave radiation, sensible and latent heat fluxes) (Hodges et al., 2000). The vertical mixing model uses the transport equations of turbulent kinetic energy (TKE) to compute the energy available from wind stirring and shear production for the mixing process (Spigel and Imberger, 1980). A complete description of the formulae and numerical methods used in ELCOM was given by Hodges et al. (2000).

Simulations of hydrodynamics of Funil reservoir were conducted with realistic forcing condition (e.g. inflow, outflow, atmospheric temperature, radiation). These simulations were aimed in order to test the hypothesis regarding the river inflows at transition zone in rainy and dry seasons in Funil reservoir. Simulations started 4 days before the date of the considered data. This is necessary to let the model equilibrate beyond the initial physical conditions. The numerical domain was discretized in a uniform horizontal grid containing 100m × 100m cells based on a depth sample. The depth data were collected from 27 to 29 February 2012. The vertical grid resolution was set to a uniform

Title Page

Abstract

Introduction

Conclusions

References

Tables

Figures

⏪

⏩

◀

▶

Back

Close

Full Screen / Esc

Printer-friendly Version

Interactive Discussion



1 m thickness, resulting in 72 vertical layers. The water albedo was set to 0.03 (Slater, 1980), and the bottom drag coefficient was set to 0.001 (Wüest and Lorke, 2003). The attenuation coefficient for PAR was set to 0.6 m^{-1} based on Secchi disc measurements. A value of $5.25 \text{ m}^2 \text{ s}^{-1}$, based on a previous study conducted in another tropical reservoir (Pacheco et al., 2011), was chosen for the horizontal diffusivity for temperature and for the horizontal momentum.

Because of the presence of persistent unstable atmospheric conditions over tropical reservoirs (Verburg and Antenucci, 2010), the atmospheric stability sub-model was activated during the simulation; this procedure is appropriate in the cases in which the meteorological sensors are located within the internal atmospheric boundary layer (ABL) over the surface of the lake and data are collected at sub-daily intervals (Imberger and Patterson, 1990). In this manner, the heat and momentum transfer coefficients were adjusted at each model time step based on the stability of the ABL. The Coriolis sub-model was also activated during the simulation.

We defined two sets of boundary cells to force the inflow (Paraíba do Sul River) and outflow: (the water intake at the dam). The meteorological driving forces over the free surface of the reservoir were considered uniform. The model was forced using hourly meteorological data acquired by SIMA, the daily inflow and outflow provided by Eletrobrás-Furnas and the cloud cover and river temperatures extracted from thermistor chain data and complemented with MODIS data. Two periods were simulated: one to represent rainy season (25 February 2012 to 4 March 2012) and one to represent dry season (15 to 23 September 2012).

3 Results

3.1 Spatial variability

Based on spatial data of Chl and $p\text{CO}_2$, a typical zonation pattern usually found in reservoirs was observed in Funil main body (riverine, transition and lacustrine zones)

BGD

11, 8531–8568, 2014

Spatial heterogeneity of Chl and CO_2 fluxes

F. S. Pacheco et al.

Title Page

Abstract

Introduction

Conclusions

References

Tables

Figures

◀

▶

◀

▶

Back

Close

Full Screen / Esc

Printer-friendly Version

Interactive Discussion



(Fig. 2). Although the boundaries are influenced by many factors and are not easily determined, these regions have distinct physical, chemical and biological features. The riverine zone (RZ) has a high input of nutrients coming from terrestrial systems and human activities, but the primary production is limited by high turbidity and turbulence. As the sedimentation and light availability increase along the reservoir, biomass of primary producers increases in the transition zone (TZ). The lacustrine zone (LZ) is characterized by nutrient limitation and reduced phytoplankton biomass (Thornton, 1990). In this study, we considered the Chl to separate the reservoir in three zones. Riverine zone is characterized by low Chl ($< 5 \mu\text{g L}^{-1}$). Transition zone begins where the Chl starts to increase and ends when Chl decrease to levels closely to Chl in Lacustrine zone. Finally, Lacustrine zone is characterized by intermediate Chl.

Funil reservoir showed to be spatially heterogeneous with seasonal differences in Chl and $p\text{CO}_2$ (Fig. 2). The spatial data showed high spatial variation only in the main body of the reservoir, while the southern part was undersaturated in CO_2 in rainy and dry seasons (Fig. 2a and b). Spatially average of $p\text{CO}_2$ for rainy and dry season were 259 ± 221 and $881 \pm 900 \mu\text{atm}$, respectively. The $p\text{CO}_2$ varied from 140 to $1376 \mu\text{atm}$ in rainy season and from 43 to $2290 \mu\text{atm}$ in dry season. Higher values of $p\text{CO}_2$ in the riverine zone of the reservoir and a drastically decrease in the transition zone were observed in both sample periods (Fig. 3a and b). In the lacustrine zone, undersaturation on CO_2 was prevalent at all sample sites in rainy and dry season. Considering all sample sites, there was significant differences between rainy and dry seasons ($t = 1.99$, $p < 0.05$) and higher values of $p\text{CO}_2$ during dry season in Funil reservoir were previously reported (Roland et al., 2010). Chl was higher in the transition zone compared with others compartments ($t = 2.01$, $p < 0.05$, Fig. 3a and b). Further, average concentration in transition zone was 2.5 times higher than the reservoir average (129.2 and $52.0 \mu\text{g L}^{-1}$, respectively). Unlike $p\text{CO}_2$, Chl data showed no significant difference between rainy and dry season considering all spatial data ($t = 1.99$, $p > 0.05$).

The calculated CO_2 fluxes from spatial data varied from -35.8 to $44.2 \text{ mmol m}^{-2} \text{ d}^{-1}$ and -47.7 to $87.3 \text{ mmol m}^{-2} \text{ d}^{-1}$ in rainy and dry season, respectively. In both rainy and

Spatial heterogeneity of Chl and CO_2 fluxes

F. S. Pacheco et al.

Title Page

Abstract

Introduction

Conclusions

References

Tables

Figures



Back

Close

Full Screen / Esc

Printer-friendly Version

Interactive Discussion



dry seasons, the maximum emission was observed in riverine zone and the minimum in the transition zone. The spatial average was -7.2 and $22.1 \text{ mmol m}^{-2} \text{ d}^{-1}$ in the rainy and dry season, respectively (Table 1).

3.2 Temporal variability

The $p\text{CO}_2$ calculated by multi-parameter sonde data (temperature and pH) and alkalinity showed a large seasonal variability over the year at the station near the dam (Table 2). The $p\text{CO}_2$ varied from 35 to 4058 μatm with average of $624 \pm 829 \mu\text{atm}$ and median of 165 μatm . The $p\text{CO}_2$ supersaturation was prevalent between April and June, while $p\text{CO}_2$ undersaturation was prevalent in all other periods (Fig. 4a). Lowest median of $p\text{CO}_2$ was observed between October and December (43 μatm). Considering all temporal data over the year, 59.8 % of the data were below atmospheric equilibrium and 1.1 % were within 5 % of atmospheric equilibrium.

In Funil Reservoir, the seasonal $p\text{CO}_2$ variation over the year at the station near the dam agreed with variation of retention time (Fig. 4). The yearly average of the reservoir retention time was 32.6 days over the considered year. Lower retention time occurs between October and December when the water level is low and the reservoir is ready to stock water coming from the watershed and rain during the rainy season (October to March).

The CO_2 flux over the year at the station near the dam varied from -119.8 to $234.5 \text{ mmol m}^{-2} \text{ d}^{-1}$. The average of flux was $-0.9 \pm 33.1 \text{ mmol m}^{-2} \text{ d}^{-1}$ and median of $-6.2 \text{ mmol m}^{-2} \text{ d}^{-1}$. We observed substantial uptake of CO_2 between October and December (rainy-spring) (Table 1). Uptake of CO_2 from the atmosphere was also prevalent between July and September (dry-winter). From January to July, the lake lost substantial CO_2 via degassing (Table 1). Summary of all other data collected over the studied period is shown in Table 2.

Spatial heterogeneity of Chl and CO_2 fluxes

F. S. Pacheco et al.

Title Page

Abstract

Introduction

Conclusions

References

Tables

Figures



Back

Close

Full Screen / Esc

Printer-friendly Version

Interactive Discussion



3.3 Thermal structure of transition zone and river

During the rainy season, thermal stratification occurred in the transition zone only during the daytime around 16:30 LT, when a maximum of 33.1 °C was observed at the surface for a minimum of 27.8 °C at the bottom (Fig. 5a); to the contrary, temperature was vertically homogeneous at nighttime. The daily range of temperature oscillation during rainy season at surface was up to 5 °C. In the dry season, water temperature were lower compared to the rainy season at transition zone. Stratification occurred around 14:00 LT in dry season, when we observed a maximum of 25.7 °C and a minimum of 23.1 °C at the bottom. The daily range of temperature oscillation was up to 3 °C at surface and stratus layers with different temperatures were observed every 2.5 m (Fig. 5b). The river temperature varied from 27.7 to 28.7 °C and 23.6 to 24.1 °C in rainy and dry season, respectively (Table 3). The average temperature difference between river and reservoir surface water was 2.1 and 0.3 °C in rainy and dry season, respectively.

3.4 Simulations

We first compared the simulated and real temperature at station S09 and S14 for rainy and dry season, respectively. The RMSE, calculated by comparing data every 20 min were 1.4 °C for rainy season and 1.1 °C for dry season. These results obtained for both seasons are comparable with previous modelling exercises found in literature (Jin et al., 2000; Vidal et al., 2012). We also analyzed the ability of the model to reproduce the inflow using data from drifters released in the river and transition zone of the reservoir on 1 March and 20 September (data not shown). Although the vertical thermal structures observed in dry season (Fig. 5b) were not well represented, the model reproduced the behavior of the inflow as underflow in rainy season (Fig. 6a) and interflow and overflow in dry season (Fig. 6b) as anticipated by the schematic representation (Fig. 5c and d). The river flowed mainly at 6 m depth near the bottom of Funil reservoir after the river plunging point in the rainy season. In the dry season, the river flowed mainly at 3 m depth at night and 4 m at daytime.

BGD

11, 8531–8568, 2014

Spatial heterogeneity of Chl and CO₂ fluxes

F. S. Pacheco et al.

Title Page

Abstract

Introduction

Conclusions

References

Tables

Figures

◀

▶

◀

▶

Back

Close

Full Screen / Esc

Printer-friendly Version

Interactive Discussion



The daily oscillation of the neutral buoyance observed occurs because of the variation of reservoir surface and river temperatures (Vidal et al., 2012; Curtarelli et al., 2013). The level of neutral buoyancy, where the densities of the flowing current and the ambient fluid are equal, represents the depth where the river water spreads laterally in the reservoir. In rainy season, the river flowed as underflow (Fig. 6a), however, when the river reached its maximum temperature around 21:00 LT (Table 3) the temperature difference between river and surface water decreased, the level of river neutral buoyance moved upward and the maximum flow was observed between 4 and 6 m (Fig. 6a). In the dry season, the river flowed as overflow, but it plunged down to 4 to 6 m depth when the high surface temperature during the day coincided with the period of lowest river temperature (Table 3) and neutral buoyance moved downward (Fig. 6b). The change in patterns observed in the river flow between 20 and 21 September occurred due to a decrease of the river temperature during a rainfall that occurred around 16:00 LT on 20 September 2012 (Fig. 6b).

4 Discussion

4.1 $p\text{CO}_2$ driven by Phytoplankton

Primary production associated to the high Chl showed to be the main regulator of CO_2 concentration at the surface of the Funil Reservoir (Fig. 7). Spatially, $p\text{CO}_2$ were negatively correlated to the Chl ($r^2 = 0.71$). In old hydropower reservoir where C source from the flooded soil after impounding has become negligible, primary production may become a significant term in the C budget. Intense primary production fuelled by high levels of nutrients reduces CO_2 concentrations to levels below atmospheric equilibrium in transition zone and lacustrine zone (Fig. 3). To the contrary, high values of $p\text{CO}_2$ in riverine zone may be associated with suspended solids and turbulence and vertical mixing that inhibit primary production.

BGD

11, 8531–8568, 2014

Spatial heterogeneity of Chl and CO_2 fluxes

F. S. Pacheco et al.

Title Page

Abstract

Introduction

Conclusions

References

Tables

Figures

◀

▶

◀

▶

Back

Close

Full Screen / Esc

Printer-friendly Version

Interactive Discussion



Spatial heterogeneity of Chl and CO₂ fluxes

F. S. Pacheco et al.

[Title Page](#)

[Abstract](#)

[Introduction](#)

[Conclusions](#)

[References](#)

[Tables](#)

[Figures](#)

[I◀](#)

[▶I](#)

[◀](#)

[▶](#)

[Back](#)

[Close](#)

[Full Screen / Esc](#)

[Printer-friendly Version](#)

[Interactive Discussion](#)



Low $p\text{CO}_2$ levels observed at the station near the dam over the year is associated with (1) high primary production due to higher temperature and solar radiation that promote water column stability and stratification, and (2) constant high nutrient availability. Since nutrient availability in Funil Reservoir is high during the entire year (Table 2), nutrients are never limited in the lacustrine zone and other factors that controls stability and stratification, such as temperature, wind and changes in mixing depth related to the seasonal variation are the main inhibitors of algal growth near the dam especially between April and June.

Due to phytoplankton productivity, we found net uptake of CO_2 over the year at the station near the dam, especially between October and December (Table 1). The fate of carbon fixed by the phytoplankton in Funil Reservoir is still unclear. The higher flux of methane (CH_4) from sediment to water found in Funil Reservoir compared to other tropical reservoir (Ometto et al., 2013) suggests that a substantial fraction of the fixed carbon reaches the sediment and is further mineralized in CH_4 . However, in lacustrine zone, the higher depth and high temperature may promote mineralization of part of carbon fixed by phytoplankton in the water column before it reaches the sediment. Outflow export the same amount of carbon that comes from the watershed (Ometto et al., 2013), so the water that flows through the turbine is not responsible to export the excess of carbon invaded from the atmosphere. Although there is no data to support this statement, as reported in natural eutrophic lakes (Downing et al., 2008), burial of organic carbon composed by phytoplankton and methanogenesis seems to be two important carbon pathways for the carbon fixed by the phytoplankton in Funil Reservoir.

4.2 Physical feature and spatial distribution

The retention time of Funil reservoir is strongly driven by the operation of the dam. The volume of water that flows through the turbine depends on the energy demands and inflow from Paraíba do Sul River. Periods of low retention time and water levels do not necessarily correspond to periods of low precipitation. In fact, highest retention time and water level is often observed in the middle of the dry season when the reservoir

is full to ensure enough water to produce energy during entire dry season. Therefore, many ecological processes in natural lakes that are related with external factor (e.g. solar radiation, precipitation and temperature) may be regulated by dam operation in hydropower reservoir.

5 The position of transition zone of the reservoir moves as result of the seasonally (Fig. 3). In the end of the rainy season, the retention time and water level was high, and the influence of the river in the surface water of the reservoir was restrict to a small area (Fig. 2a and c). Differently, when the water level and retention time was low, the transition zone moved toward the dam and the river inflow influenced the surface Chl and $p\text{CO}_2$ in more than 40 % of the total reservoir surface area (Fig. 2b and d). A reservoir can become a fluvial-dominated system when retention time is short or lacustrine when retention time is long (Straškraba, 1990).

10 Size of the river-influenced area in the reservoir surface water also depends on water density. Differences on river and reservoir temperature, total dissolved solids, and suspended solids can cause density gradient in the water column. Depending on the water density differences between the inflow and reservoir, the river can flow into the downstream area as overflow, underflow, or interflow (Martin and McCutcheon, 1998). During the rainy season in Funil reservoir, due to the high difference between river and reservoir surface temperature ($\sim 4^\circ\text{C}$), the river water progressively sinks down (underflow), and contributes to the thermal stability of the water column (Fig. 5a, Assireu et al., 2011). The denser river water flows under a lighter reservoir water and waves and billows develops along the interface due to shear velocity. This behavior is indicative of the Kelvin–Helmholtz instability, in which waves made up of fluid from the current (river) promote mixing with the reservoir water (Thorpe and Jiang, 1998; Corcos and Sherman, 2005) (Fig. 5c). This mixing and the high nutrient concentration coming from Paraíba do Sul River (Table 2) may explain the high levels of Chlorophyll *a* observed in the transition zone (Fig. 3).

25 Many cold fronts pass through Brazilian middle-west and southeast in dry seasons. (Lorenzetti et al., 2005; Alcântara et al., 2010). Thus, the decrease of reservoir surface

BGD

11, 8531–8568, 2014

Spatial heterogeneity of Chl and CO_2 fluxes

F. S. Pacheco et al.

Title Page

Abstract

Introduction

Conclusions

References

Tables

Figures

◀

▶

◀

▶

Back

Close

Full Screen / Esc

Printer-friendly Version

Interactive Discussion



Spatial heterogeneity of Chl and CO₂ fluxes

F. S. Pacheco et al.

Title Page

Abstract

Introduction

Conclusions

References

Tables

Figures

◀

▶

◀

▶

Back

Close

Full Screen / Esc

Printer-friendly Version

Interactive Discussion



temperature (Table 2) and consequent decrease in density difference between river and reservoir surface leads to river inflow characterized by inter-overflow (Fig. 5b and d). In an inter-overflow, the riverine characteristic of high turbulence, $p\text{CO}_2$ and low Chl is observed in the reservoir surface 5 km toward the dam (Fig. 3a and b). Although there is high nutrient concentrations in the transition zone (Table 1) between S19 and the river, the surface water is dominated by river flow with low Chl concentrations (Fig. 3). Phytoplankton will not bloom until they get a certain distance down-reservoir and the inflow mixes with the reservoir and loses velocity (Vidal et al., 2012).

The ELCOM simulations using real data represented the river inflow during the rainy and dry season (Fig. 6). The results converge to the conclusion of a lower influence of the river on surface waters during the rainy season since a higher dense (colder and more turbid) river plunges when reach a warmer reservoir water. Although the model does not represented the intrusions of river water on different depths (every 2.5 m) suggested by temperature profile at transition zone in dry season (Fig. 5b), the model represented the overflow, especially at night (Fig. 6). The daily scale variation of the river inflow (Fig. 6) occur as response of the lagged change of temperature of the river and reservoir over the day. In rainy season, this oscillation facilitate the injection of nutrient in euphotic zone when the reservoir surface temperature decreases and river temperature reaches its maximum in the end of the day (Table 3). During the day, when the river temperature drops, the large peak of Chl in transition zone (Fig. 3a) could be result of diurnal stratification developing (Fig. 5). In dry season, the peak of Chl occurs five kilometers further downstream (Fig. 3b), since inflow never plunges due to lower temperature differences between river and reservoir surface.

4.3 Spatial and temporal heterogeneity

As a result of phytoplankton growth associated with these physical features, there are large spatial and temporal variation of CO₂ fluxes in the Funil Reservoir. Several studies of hydropower reservoir have suggested that significant CO₂ evade from these systems to the atmosphere at a global scale (St Louis et al., 2000; Roehm and Tremblay, 2006;

Spatial heterogeneity of Chl and CO₂ fluxes

F. S. Pacheco et al.

[Title Page](#)[Abstract](#)[Introduction](#)[Conclusions](#)[References](#)[Tables](#)[Figures](#)[I◀](#)[▶I](#)[◀](#)[▶](#)[Back](#)[Close](#)[Full Screen / Esc](#)[Printer-friendly Version](#)[Interactive Discussion](#)

Barros et al., 2011; Fearnside and Pueyo, 2012). However, recent studies have shown that the growing nutrient enrichment caused by human activities (eutrophication) can reverse this pattern in some hydropower reservoir (Roland et al., 2010) and natural lakes (Pacheco et al., 2014). Our study shows that Funil reservoir is spatially heterogeneous with high CO₂ emission in riverine zone and high CO₂ uptake in transition and lacustrine zone. Temporally, the reservoir near the dam is undersaturated in $p\text{CO}_2$ mainly between October and December, and supersaturated in $p\text{CO}_2$ between April and June (Table 1).

We might have different or opposite conclusions if spatial and temporal $p\text{CO}_2$ data are analyzed separately. Previous studies suggested that in natural small lakes, a single sample site should be adequate to determine if a lake is above or below equilibrium with the atmosphere and the intensity of the fluxes (Kelly et al., 2001). However, large spatial heterogeneity, regarding $p\text{CO}_2$ and CO₂ emission to atmosphere, was observed in boreal (Teodoru et al., 2011) and tropical (Roland et al., 2010) reservoir. Our temporal data at the dam station showed lower $p\text{CO}_2$ over October, November and December when the retention time is extremely low (Table 4), but this observation does not represent the entire reservoir. The spatial data collected at low water level showed low $p\text{CO}_2$ in the dam as well, however almost half reservoir is supersaturated due to the river influence (Fig. 2d). The average $p\text{CO}_2$ during low retention time was 881 μatm considering whole reservoir area, contrasting with only 69 μatm near the dam. Furthermore, if we considered only one station near the dam to estimate CO₂ flux between lake surface and atmosphere, the conclusion would be contradictory. For example, in periods of low retention time, calculated CO₂ flux shows that CO₂ flux would be $-17.6 \text{ mmol m}^{-2} \text{ d}^{-1}$ (CO₂ sink) considering one spot temporal data, and $22.1 \text{ mmol m}^{-2} \text{ d}^{-1}$ (CO₂ source) considering whole reservoir (Table 4).

Same contradictory conclusion can be found when studies with low number of sample sites are considered in the spatial heterogeneity discussion. Previous studies about heterogeneity considering four stations in Funil reservoir showed that peak of phytoplankton biomass in transition zone was not observed (Soares et al., 2012). However,

our Chl data collected every 1000 m, proximally, showed a clear transition zone with peaks of Chl. Furthermore, data analysis from only four stations showed that high spatial heterogeneity occurs in periods of high retention time (high water level). To the contrary, our data reveal high spatial heterogeneity in low retention time, corresponding to periods with high influence of the river in the surface water. Different conclusions found by Soares et al. (2012) may be explained by the variation of transition zone location. This zone is limited to a small area and its location varies depending on retention time and inflow (Fig. 2c and d). Therefore, low number of sample stations in Funil reservoir showed to limit the capacity to represent whole reservoir and to discuss about spatial heterogeneity. Since high number of stations and variables increases fieldwork time and costs, a balance between them must be considered to ensure acceptable representativeness.

5 Conclusion

In summary, the seasonal and spatial variability of Chl and CO₂ fluxes in Funil reservoir is mainly related to river inflow and retention time. However, the relationship between $p\text{CO}_2$ and Chl suggests that primary production regulates surface CO₂ fluxes in transition and lacustrine zone. Average of spatial data showed CO₂ evasion to the atmosphere in periods of low retention time (even with higher Chl) due to river influence on water surface, and CO₂ uptake in periods of high retention time when the river plunges and flows under the reservoir. However, the threshold of retention time that seal the transition between source and sink of CO₂ could not be determined. Comparison between spatial (42 stations) and temporal data (one station) showed that different conclusions can be drawn if spatial heterogeneity is not adequately considered. Moreover, change of transition zone location over the year must be considered when low number of stations is used to represent spatial heterogeneity. Lack of spatial information of CO₂ flux could lead to erroneous conclusion of the importance of hydropower reservoir to freshwater carbon cycle. Funil reservoir is a dynamic system where the

BGD

11, 8531–8568, 2014

Spatial heterogeneity of Chl and CO₂ fluxes

F. S. Pacheco et al.

Title Page

Abstract

Introduction

Conclusions

References

Tables

Figures

◀

▶

◀

▶

Back

Close

Full Screen / Esc

Printer-friendly Version

Interactive Discussion



hydrodynamics linked to river inflow and retention time controls both $p\text{CO}_2$ and Chl spatial variability and seems to be the key that regulate most of ecological process.

Acknowledgements. This work was supported by the project “Carbon Budgets of Hydroelectric Reservoirs of Furnas Centrais Elétricas S. A.”. Thanks to the Center for Water Research (CWR) and its director, Jörg Imberger, for making ELCOM available for this study. We also thank the São Paulo State Science Foundation for financial support (FAPESP process no. 2010/06869-0). GA is a visiting special researcher from the Brazilian CNPq program Ciência Sem Fronteiras (process #401726/2012-6).

References

Abril, G., Guerin, F., Richard, S., Delmas, R., Galy-Lacaux, C., Gosse, P., Tremblay, A., Varfalvy, L., Dos Santos, M. A., and Matvienko, B.: Carbon dioxide and methane emissions and the carbon budget of a 10 year old tropical reservoir (Petit Saut, French Guiana), *Global Biogeochem. Cy.*, 19, GB4007, doi:10.1029/2005gb002457, 2005.

Abril, G., Richard, S., and Guerin, F.: In situ measurements of dissolved gases (CO_2 and CH_4) in a wide range of concentrations in a tropical reservoir using an equilibrator, *Sci. Total Environ.*, 354, 246–251, doi:10.1016/j.scitotenv.2005.12.051, 2006.

Abril, G., Parize, M., Perez, M. A. P., and Filizola, N.: Wood decomposition in Amazonian hydropower reservoirs: an additional source of greenhouse gases, *J. S. Am. Earth Sci.*, 44, 104–107, doi:10.1016/j.jsames.2012.11.007, 2013.

Abril, G., Martinez, J.-M., Artigas, L. F., Moreira-Turcq, P., Benedetti, M. F., Vidal, L., Meziane, T., Kim, J.-H., Bernardes, M. C., Savoye, N., Deborde, J., Souza, E. L., Alberic, P., Landim de Souza, M. F., and Roland, F.: Amazon River carbon dioxide outgassing fuelled by wetlands, *Nature*, 505, 395–398, doi:10.1038/nature12797, 2014.

AGEVAP: Relatório Técnico – Bacia do Rio Paraíba Do Sul – Subsídios às Ações de Melhoria da Gestão 2011, Associação Pró-Gestão das Águas da Bacia Hidrográfica do Rio Paraíba do Sul, 255, Resende, 2011.

Akaike, H.: New look at statistical-model identification, *IEEE T. Automat. Contr.*, AC19, 716–723, doi:10.1109/tac.1974.1100705, 1974.

Alcântara, E. H., Bonnet, M. P., Assireu, A. T., Stech, J. L., Novo, E. M. L. M., and Lorenzetti, J. A.: On the water thermal response to the passage of cold fronts: initial

Spatial heterogeneity of Chl and CO_2 fluxes

F. S. Pacheco et al.

Title Page

Abstract

Introduction

Conclusions

References

Tables

Figures

◀

▶

◀

▶

Back

Close

Full Screen / Esc

Printer-friendly Version

Interactive Discussion



Spatial heterogeneity of Chl and CO₂ fluxes

F. S. Pacheco et al.

[Title Page](#)

[Abstract](#)

[Introduction](#)

[Conclusions](#)

[References](#)

[Tables](#)

[Figures](#)

[I ◀](#)

[▶ I](#)

[◀](#)

[▶](#)

[Back](#)

[Close](#)

[Full Screen / Esc](#)

[Printer-friendly Version](#)

[Interactive Discussion](#)



results for Itumbiara reservoir (Brazil), *Hydrol. Earth Syst. Sci. Discuss.*, 7, 9437–9465, doi:10.5194/hessd-7-9437-2010, 2010.

Alcantara, E., Curtarelli, M., Ogashawara, I., Stech, J., and Souza, A.: Hydrographic observations at SIMA station Itumbiara in 2013, in: *Long-term Environmental Time Series of Continuously Collected Data in Hydroelectric Reservoirs in Brazil*, edited by: Alcantara, E., Curtarelli, M., Ogashawara, I., Stech, J., and Souza, A., PANGAEA, Bremerhaven, 1–3, 2013.

APHA: *Standard Methods for the Examination of Water and Wastewater*, 21 ed., Washington, DC, 1368 pp., 2005.

Assireu, A. T., Alcântara, E., Novo, E. M. L. M., Roland, F., Pacheco, F. S., Stech, J. L., and Lorenzetti, J. A.: Hydro-physical processes at the plunge point: an analysis using satellite and in situ data, *Hydrol. Earth Syst. Sci.*, 15, 3689–3700, doi:10.5194/hess-15-3689-2011, 2011.

Bailey, T. C. and Gatrell, A. C.: *Interactive Spatial Data Analysis*, Longman Scientific & Technical, Essex, 1995.

Barros, N., Cole, J. J., Tranvik, L. J., Prairie, Y. T., Bastviken, D., Huszar, V. L. M., del Giorgio, P., and Roland, F.: Carbon emission from hydroelectric reservoirs linked to reservoir age and latitude, *Nat. Geosci.*, 4, 593–596, doi:10.1038/Ngeo1211, 2011.

Borges, A. V., Vanderborght, J.-P., Schiettecatte, L. S., Gazeau, F., Ferrón-Smith, S., Delille, B., and Frankignoulle, M.: Variability of the gas transfer velocity of CO₂ in a macrotidal estuary (the Scheldt), *Estuaries*, 27, 593–603, doi:10.1007/BF02907647, 2004.

Branco, C. W. C., Rocha, M. I. A., Pinto, G. F. S., Gômara, G. A., and Filippo, R.: Limnological features of Funil Reservoir (R. J., Brazil) and indicator properties of rotifers and cladocerans of the zooplankton community, *Lakes & Reservoirs: Research & Management*, *Lakes Reserv. Res. Manag.*, 7, 87–92, doi:10.1046/j.1440-169X.2002.00177.x, 2002.

Câmara, G., Souza, R. C. M., Freitas, U. M., and Garrido, J.: Spring: Integrating remote sensing and gis by object-oriented data modelling, *Comput. Graph.*, 20, 395–403, doi:10.1016/0097-8493(96)00008-8, 1996.

Casulli, V. and Cheng, R. T.: Semiimplicit finite-difference methods for 3-dimensional shallow-water flow, *Int. J. Numer. Meth. Fl.*, 15, 629–648, doi:10.1002/flid.1650150602, 1992.

Cole, J. J. and Caraco, N. F.: Atmospheric exchange of carbon dioxide in a low-wind oligotrophic lake measured by the addition of SF₆, *Limnol. Oceanogr.*, 43, 647–656, 1998.

**Spatial heterogeneity
of Chl and CO₂ fluxes**

F. S. Pacheco et al.

[Title Page](#)[Abstract](#)[Introduction](#)[Conclusions](#)[References](#)[Tables](#)[Figures](#)[I◀](#)[▶I](#)[◀](#)[▶](#)[Back](#)[Close](#)[Full Screen / Esc](#)[Printer-friendly Version](#)[Interactive Discussion](#)

- Corcos, G. M. and Sherman, F. S.: The mixing layer: deterministic models of a turbulent flow, *J. Fluid. Mech.*, 139, 29–65, 2005.
- Demarty, M., Bastien, J., and Tremblay, A.: Annual follow-up of gross diffusive carbon dioxide and methane emissions from a boreal reservoir and two nearby lakes in Québec, Canada, *Biogeosciences*, 8, 41–53, doi:10.5194/bg-8-41-2011, 2011.
- Di Siervi, M. A., Mariazzi, A. A., and Donadelli, J. L.: Bacterioplankton and phytoplankton production in a large Patagonian reservoir (Republica Argentina), *Hydrobiologia*, 297, 123–129, 1995.
- Downing, J. A., Cole, J. J., Middelburg, J. J., Striegl, R. G., Duarte, C. M., Kortelainen, P., Prairie, Y. T., and Laube, K. A.: Sediment organic carbon burial in agriculturally eutrophic impoundments over the last century, *Global Biogeochem. Cy.*, 22, Gb1018, doi:10.1029/2006gb002854, 2008.
- Fearnside, P. M. and Pueyo, S.: Greenhouse-gas emissions from tropical dams, *Nature Clim. Change*, 2, 382–384, 2012.
- Finlay, K., Leavitt, P. R., Wissel, B., and Prairie, Y. T.: Regulation of spatial and temporal variability of carbon flux in six hard-water lakes of the northern Great Plains, *Limnol. Oceanogr.*, 54, 2553–2564, doi:10.4319/lo.2009.54.6_part_2.2553, 2009.
- Finlay, K., Leavitt, P. R., Patoine, A., and Wissel, B.: Magnitudes and controls of organic and inorganic carbon flux through a chain of hard-water lakes on the northern Great Plains, *Limnol. Oceanogr.*, 55, 1551–1564, doi:10.4319/lo.2010.55.4.1551, 2010.
- Fischer, H. B. and Smith, R. D.: Observations of transport to surface waters from a plunging inflow to Lake Mead, *Limnol. Oceanogr.*, 28, 258–272, 1983.
- Fischer, H. B., List, E. J., Koh, R. C. Y., Imberger, J., and Brooks, N. H.: *Mixing in Inland and Coastal Waters*, Academic Press, New York, 483 pp., 1979.
- Ford, D. E.: Reservoir transport processes, in: *Reservoir Limnology: Ecological Perspectives*, edited by: Thornton, K. W., Kimmel, B. L., and Payne, F. E., Wiley-Interscience, New York, 15–41, 1990.
- Gippel, C. J.: The use of turbidimeters in suspended sediment research, *Hydrobiologia*, 176, 465–480, doi:10.1007/bf00026582, 1989.
- Halbedel, S. and Koschorreck, M.: Regulation of CO₂ emissions from temperate streams and reservoirs, *Biogeosciences*, 10, 7539–7551, doi:10.5194/bg-10-7539-2013, 2013.
- Hodges, B. R., Imberger, J., Saggio, A., and Winters, K. B.: Modeling basin-scale internal waves in a stratified lake, *Limnol. Oceanogr.*, 45, 1603–1620, 2000.

- IBGE: Instituto Brasileiro de Geografia e Estatística, Censo Demográfico 2010, Rio de Janeiro, 2010.
- Imberger, J. and Patterson, J. C.: Physical limnology, *Adv. Appl. Mech.*, 27, 303–475, 1990.
- Jahne, B., Munnich, K. O., Bosinger, R., Dutzi, A., Huber, W., and Libner, P.: On the parameters influencing air-water gas-exchange, *J. Geophys. Res.-Oceans*, 92, 1937–1949, doi:10.1029/JC092iC02p01937, 1987.
- Jin, K., Hamrick, J., and Tisdale, T.: Application of three-dimensional hydrodynamic model for Lake Okeechobee, *J. Hydraul. Eng.*, 126, 758–771, doi:10.1061/(ASCE)0733-9429(2000)126:10(758), 2000.
- Kelly, C. A., Fee, E., Ramlal, P. S., Rudd, J. W. M., Hesslein, R. H., Anema, C., and Schindler, E. U.: Natural variability of carbon dioxide and net epilimnetic production in the surface waters of boreal lakes of different sizes, *Limnol. Oceanogr.*, 46, 1054–1064, 2001.
- Kemenes, A., Forsberg, B. R., and Melack, J. M.: CO₂ emissions from a tropical hydroelectric reservoir (Balbina, Brazil), *J. Geophys. Res.-Biogeo.*, 116, G03004, doi:10.1029/2010jg001465, 2011.
- Kennedy, R. H.: Reservoir design and operation: limnological implications and management opportunities, in: *Theoretical Reservoir Ecology and its Applications*, edited by: Tundisi, J. G. and Straškraba, M., Backhuys Publishers, Leiden, 1–28, 1999.
- Klapper, H.: Water quality problems in reservoirs of Rio de Janeiro, Minas Gerais and Sao Paulo, *Int. Rev. Hydrobiol.*, 83, 93–101, 1998.
- Lauster, G. H., Hanson, P. C., and Kratz, T. K.: Gross primary production and respiration differences among littoral and pelagic habitats in northern Wisconsin lakes, *Can. J. Fish. Aquat. Sci.*, 63, 1130–1141, doi:10.1139/f06-018, 2006.
- Leonard, B. P.: The ultimate conservative difference scheme applied to unsteady one-dimensional advection, *Comput. Method. Appl. M.*, 88, 17–74, doi:10.1016/0045-7825(91)90232-U, 1991.
- Lorenzetti, J. A., Stech, J. L., Assireu, A. T., Novo, E. M. L. D., and Lima, I. B. T.: SIMA: a near real time buoy acquisition and telemetry system as a support for limnological studies, in: *Global Warming and Hydroelectric Reservoirs.*, edited by: Santos, M. A. and Rosa, L. P., COPPE, Rio de Janeiro, 71–79, 2005.
- Martin, J. L. and McCutcheon, S. C.: *Hydrodynamics and Transport for Water Quality Modeling*, CRC Press, Boca Raton, 1998.

Spatial heterogeneity of Chl and CO₂ fluxes

F. S. Pacheco et al.

[Title Page](#)[Abstract](#)[Introduction](#)[Conclusions](#)[References](#)[Tables](#)[Figures](#)[I ◀](#)[▶ I](#)[◀](#)[▶](#)[Back](#)[Close](#)[Full Screen / Esc](#)[Printer-friendly Version](#)[Interactive Discussion](#)

**Spatial heterogeneity
of Chl and CO₂ fluxes**

F. S. Pacheco et al.

[Title Page](#)[Abstract](#)[Introduction](#)[Conclusions](#)[References](#)[Tables](#)[Figures](#)[I ◀](#)[▶ I](#)[◀](#)[▶](#)[Back](#)[Close](#)[Full Screen / Esc](#)[Printer-friendly Version](#)[Interactive Discussion](#)

- 5 Millero, F. J., Pierrot, D., Lee, K., Wanninkhof, R., Feely, R., Sabine, C. L., Key, R. M., and Takahashi, T.: Dissociation constants for carbonic acid determined from field measurements, *Deep-Sea Res. Pt. I.*, 49, 1705–1723, doi:10.1016/s0967-0637(02)00093-6, 2002.
- 10 Ometto, J. P. H. B., Pacheco, F. S., Cimberlis, A. C. P., Stech, J. L., Lorenzetti, J., Assireu, A. T., Santos, M. A., Matvienko, B., Rosa, L. P., Sadigisgalli, C., Donato, A., Tundisi, J. G., Barros, N. O., Mendonca, R., and Roland, F.: Carbon dynamic and emissions in Brazilian hydropower reservoirs, in: *Energy Resources: Development, Distribution and Exploitation*, edited by: Alcantara, E., Nova Science Publishers, Hauppauge, 155–188, 2011.
- 15 Ometto, J. P., Cimberlis, A. C. P., dos Santos, M. A., Rosa, L. P., Abe, D., Tundisi, J. G., Stech, J. L., Barros, N., and Roland, F.: Carbon emission as a function of energy generation in hydroelectric reservoirs in Brazilian dry tropical biome, *Energ. Policy*, 58, 109–116, doi:10.1016/j.enpol.2013.02.041, 2013.
- Pacheco, F. S., Assireu, A. T., and Roland, F.: Drifters tracked by satellite applied to freshwater ecosystems: study case in Manso Reservoir, in: *New Technologies for the Monitoring and Study of Large Hydroelectric Reservoirs and Lakes*, edited by: Alcantara, E. H., Stech, J. L., and Novo, E. M. L. M., Parêntese, Rio de Janeiro, 193–218, 2011.
- 20 Pacheco, F. S., Roland, F., and Downing, J. A.: Eutrophication reverses whole-lake carbon budgets, *Inland Waters*, 4, 41–48, doi:10.5268/iw-4.1.614, 2014.
- Rangel, L. M., Silva, L. H. S., Rosa, P., Roland, F., and Huszar, V. L. M.: Phytoplankton biomass is mainly controlled by hydrology and phosphorus concentrations in tropical hydroelectric reservoirs, *Hydrobiologia*, 693, 13–28, doi:10.1007/s10750-012-1083-3, 2012.
- Richardot, M., Debroas, D., Jugnia, L. B., Tadonleke, R., Berthon, L., and Devaux, J.: Changes in bacterial processing and composition of dissolved organic matter in a newly-flooded reservoir (a three-year study), *Arch. Hydrobiol.*, 148, 231–248, 2000.
- 25 Rocha, M. I. A., Branco, C. W. C., Sampaio, G. F., Gômara, G. A., and de Filippo, R.: Spatial and temporal variation of limnological features, *Microcystis aeruginosa* and zooplankton in a eutrophic reservoir (Funil Reservoir, Rio de Janeiro), *Acta Limnol. Bras.*, 14, 73–86, 2002.
- Roehm, C. and Tremblay, A.: Role of turbines in the carbon dioxide emissions from two boreal reservoirs, Quebec, Canada, *J. Geophys. Res.-Atmos.*, 111, 9, doi:10.1029/2006jd007292, 2006.
- 30 Roland, F., Vidal, L. O., Pacheco, F. S., Barros, N. O., Assireu, A., Ometto, J. P. H. B., Cimberlis, A. C. P., and Cole, J. J.: Variability of carbon dioxide flux from tropical (Cerrado) hydroelectric reservoirs, *Aquat. Sci.*, 72, 283–293, doi:10.1007/s00027-010-0140-0, 2010.

Spatial heterogeneity of Chl and CO₂ fluxes

F. S. Pacheco et al.

[Title Page](#)

[Abstract](#)

[Introduction](#)

[Conclusions](#)

[References](#)

[Tables](#)

[Figures](#)

[I◀](#)

[▶I](#)

[◀](#)

[▶](#)

[Back](#)

[Close](#)

[Full Screen / Esc](#)

[Printer-friendly Version](#)

[Interactive Discussion](#)



- Rosa, L. P., dos Santos, M. A., Matvienko, B., dos Santos, E. O., and Sikar, E.: Greenhouse gas emissions from hydroelectric reservoirs in tropical regions, *Climatic Change*, 66, 9–21, doi:10.1023/B:Clim.0000043158.52222.Ee, 2004.
- Serra, T., Vidal, J., Casamitjana, X., Soler, M., and Colomer, J.: The role of surface vertical mixing in phytoplankton distribution in a stratified reservoir, *Limnol. Oceanogr.*, 52, 620–634, 2007.
- Slater, P. G.: *Remote Sensing, Optics and Optical Systems*, Addison-Wesley Pub. Co., Reading, 575 pp., 1980.
- Smith, S. V.: Physical, chemical and biological characteristics of CO₂ gas flux across the air water interface, *Plant Cell Environ.*, 8, 387–398, doi:10.1111/j.1365-3040.1985.tb01674.x, 1985.
- Soares, M. C. S., Marinho, M. M., Huszar, V. L. M., Branco, C. W. C., and Azevedo, S. M. F. O.: The effects of water retention time and watershed features on the limnology of two tropical reservoirs in Brazil, *Lakes Reserv. Res. Manag.*, 13, 257–269, doi:10.1111/j.1440-1770.2008.00379.x, 2008.
- Soares, M. C. S., Marinho, M. M., Azevedo, S. M. O. F., Branco, C. W. C., and Huszar, V. L. M.: Eutrophication and retention time affecting spatial heterogeneity in a tropical reservoir, *Limnologia*, 42, 197–203, doi:10.1016/j.limno.2011.11.002, 2012.
- Spigel, R. H. and Imberger, J.: The classification of mixed-layer dynamics in lakes of small to medium size, *J. Phys. Oceanogr.*, 10, 1104–1121, doi:10.1175/1520-0485(1980)010<1104:Tcomld>2.0.Co;2, 1980.
- St Louis, V. L., Kelly, C. A., Duchemin, E., Rudd, J. W. M., and Rosenberg, D. M.: Reservoir surfaces as sources of greenhouse gases to the atmosphere: a global estimate, *Bioscience*, 50, 766–775, 2000.
- Stevenson, M. R., Lorenzetti, J. A., Stech, J. L., and Arlino, P. R. A.: SIMA – an Integrated Environmental Monitoring System, VII Simpósio Brasileiro de Sensoriamento Remoto, Curitiba, 10–14 May 1993, 1993.
- Straškraba, M.: Retention time as a key variable of reservoir limnology, in: *Theoretical Reservoir Ecology and its Applications*, edited by: Tundisi, T. G. and Straškraba, M., Backhuys Publishers, Leiden, 43–70, 1990.
- Teodoru, C. R., Prairie, Y. T., and del Giorgio, P. A.: Spatial heterogeneity of surface CO₂ fluxes in a newly created eastmain-1 reservoir in northern Quebec, Canada, *Ecosystems*, 14, 28–46, doi:10.1007/s10021-010-9393-7, 2011.

**Spatial heterogeneity
of Chl and CO₂ fluxes**

F. S. Pacheco et al.

[Title Page](#)[Abstract](#)[Introduction](#)[Conclusions](#)[References](#)[Tables](#)[Figures](#)[I◀](#)[▶I](#)[◀](#)[▶](#)[Back](#)[Close](#)[Full Screen / Esc](#)[Printer-friendly Version](#)[Interactive Discussion](#)

- Thorpe, S. A. and Jiang, R.: Estimating internal waves and diapycnal mixing from conventional mooring data in a lake, *Limnol. Oceanogr.*, 43, 936–945, 1998.
- Verburg, P. and Antenucci, J. P.: Persistent unstable atmospheric boundary layer enhances sensible and latent heat loss in a tropical great lake: Lake Tanganyika, *J. Geophys. Res.-Atmos.*, 115, D11109, doi:10.1029/2009jd012839, 2010.
- Vidal, J., Marce, R., Serra, T., Colomer, J., Rueda, F., and Casamitjana, X.: Localized algal blooms induced by river inflows in a canyon type reservoir, *Aquat. Sci.*, 74, 315–327, doi:10.1007/s00027-011-0223-6, 2012.
- Wanninkhof, R.: Relationship between wind-speed and gas-exchange over the ocean, *J. Geophys. Res.-Oceans*, 97, 7373–7382, doi:10.1029/92jc00188, 1992.
- Weiss, R. F.: Carbon dioxide in water and seawater: the solubility of a non-ideal gas, *Mar. Chem.*, 2, 203–215, 1974.
- Wetzel, R. G. and Likens, G. E.: *Limnological Analyses*, Springer, New York, 2000.
- Wüest, A. and Lorke, A.: Small-scale hydrodynamics in lakes, *Annu. Rev. Fluid. Mech.*, 35, 373–412, doi:10.1146/annurev.fluid.35.101101.161220, 2003.
- Zhao, Y., Wu, B. F., and Zeng, Y.: Spatial and temporal patterns of greenhouse gas emissions from Three Gorges Reservoir of China, *Biogeosciences*, 10, 1219–1230, doi:10.5194/bg-10-1219-2013, 2013.

Spatial heterogeneity of Chl and CO₂ fluxes

F. S. Pacheco et al.

[Title Page](#)[Abstract](#)[Introduction](#)[Conclusions](#)[References](#)[Tables](#)[Figures](#)[I◀](#)[▶I](#)[◀](#)[▶](#)[Back](#)[Close](#)[Full Screen / Esc](#)[Printer-friendly Version](#)[Interactive Discussion](#)**Table 1.** Average CO₂ fluxes (mmol m⁻² d⁻¹) calculated using spatial and temporal data. Positive fluxes denotes net gas fluxes from the lake to the atmosphere.

| | CO ₂ fluxes mmol m ⁻² d ⁻¹ | |
|--------------------------|---|-----------|
| | Average | Std. Dev. |
| Spatial data | | |
| Rainy – Summer | | |
| Entire Reservoir | -7.20 | 21.87 |
| Riverine Zone | 37.64 | 5.46 |
| Transition Zone | -19.10 | 11.74 |
| Lacustrine Zone | -14.07 | 6.99 |
| Dry – Winter | | |
| Entire Reservoir | 22.14 | 50.78 |
| Riverine Zone | 78.74 | 11.23 |
| Transition Zone | -2.01 | 42.09 |
| Lacustrine Zone | -22.87 | 13.90 |
| Temporal data at the Dam | | |
| Over the year | -0.9 | 33.1 |
| Rainy – Spring | -27.08 | 18.50 |
| Rainy – Summer | 7.61 | 35.55 |
| Dry – Autumn | 19.63 | 29.85 |
| Dry – Winter | -0.57 | 25.47 |

Spatial heterogeneity of Chl and CO₂ fluxes

F. S. Pacheco et al.

Table 2. Average and standard deviation of environmental and chemical variable from the station S28 (near the dam) and river. ^a Cumulative precipitation over three months.

| Months Season | Oct–Dec | | Jan–Mar | | Apr–Jun | | Jul–Sep | |
|---|-----------------|--------------------|-----------------|--------------------|---------------|--------------------|---------------|--------------------|
| | Rainy – Average | Spring – Std. Dev. | Rainy – Average | Summer – Std. Dev. | Dry – Average | Autumn – Std. Dev. | Dry – Average | Winter – Std. Dev. |
| Air temperature (°C) | 22.5 | 4.0 | 24.0 | 3.3 | 20.7 | 3.1 | 19.6 | 4.0 |
| Alkalinity (mg L ⁻¹ as CaCO ₃) | 11.0 | 0.2 | 15.5 | 4.6 | 11.3 | 3.7 | 12.5 | 3.0 |
| Chlorophyll (mg L ⁻¹) | 12.9 | 12.8 | 23.8 | 20.6 | 3.0 | 0.2 | 23.2 | 35.0 |
| Total Phosphorus (µg L ⁻¹) | 42.3 | 8.5 | 41.7 | 12.2 | 18.4 | 8.6 | 33.7 | 28.0 |
| Total Nitrogen (µg L ⁻¹) | 1264.6 | 357.1 | 1143.2 | 305.3 | 1505.6 | 454.3 | 1203.3 | 299.7 |
| Maximum Depth (m) | 65.1 | 1.8 | 69.3 | 1.4 | 71.6 | 2.5 | 69.1 | 4.4 |
| Mean Reservoir Depth (m) | 19.3 | 0.4 | 20.3 | 0.4 | 20.9 | 0.7 | 20.3 | 1.1 |
| pCO ₂ (µatm) | 68.9 | 118.6 | 848.9 | 1027.5 | 1111.8 | 907.5 | 521.9 | 618.5 |
| Precipitation (mm) ^a | 547.0 | | 420.2 | | 230.2 | | 71.6 | |
| Retention Time (days) | 27.9 | 7.7 | 33.0 | 9.0 | 36.4 | 6.4 | 33.2 | 7.4 |
| Max Daily Solar Radiation (W m ⁻²) | 937.7 | 276.1 | 958.1 | 246.8 | 716.9 | 227.2 | 758.0 | 189.7 |
| Surface Water temperature (°C) | 24.7 | 1.1 | 27.1 | 1.0 | 24.1 | 1.7 | 22.0 | 1.0 |
| Wind Speed (m s ⁻¹) | – | – | 1.6 | 1.2 | 1.4 | 1.3 | 1.6 | 1.5 |
| River Total Phosphorus (mg L ⁻¹) | 80.6 | – | 77.1 | – | 42.4 | – | 88.3 | – |
| River Total Nitrogen (mg L ⁻¹) | 1535.5 | – | 2072.5 | – | 1524.2 | – | 1972.6 | – |
| Inflow (m ³ s ⁻¹) | 224.2 | 58.9 | 236.4 | 74.1 | 234.1 | 36.7 | 168.9 | 28.7 |
| Outflow (m ³ s ⁻¹) | 223.6 | 57.2 | 236.4 | 74.1 | 226.0 | 30.9 | 219.1 | 10.7 |

Title Page

Abstract

Introduction

Conclusions

References

Tables

Figures

I ◀

▶ I

◀

▶

Back

Close

Full Screen / Esc

Printer-friendly Version

Interactive Discussion



Table 3. Profile's average of the hourly river temperature collected by thermistor chain located at station S05 on 29 February 2012 (rainy season) and 20 September 2012 (dry season).

| rainy season | | | | | |
|--------------|--------------------|-----------|----------|------------------|-----------|
| Hour | River Temp. (°C) | | Hour | River Temp. (°C) | |
| | Average | Std. Dev. | | Average | Std. Dev. |
| 00:00 LT | 28.39 | 0.04 | 12:00 LT | 27.71 | 0.03 |
| 01:00 LT | 28.28 | 0.04 | 13:00 LT | 27.72 | 0.04 |
| 02:00 LT | 28.17 | 0.05 | 14:00 LT | 27.79 | 0.11 |
| 03:00 LT | 28.07 | 0.03 | 15:00 LT | 27.97 | 0.06 |
| 04:00 LT | 28.00 | 0.02 | 16:00 LT | 28.03 | 0.02 |
| 05:00 LT | 27.91 | 0.04 | 17:00 LT | 28.16 | 0.09 |
| 06:00 LT | 27.85 | 0.04 | 18:00 LT | 28.34 | 0.09 |
| 07:00 LT | 27.77 | 0.05 | 19:00 LT | 28.49 | 0.06 |
| 08:00 LT | 27.73 | 0.00 | 20:00 LT | 28.63 | 0.04 |
| 09:00 LT | 27.72 | 0.01 | 21:00 LT | 28.70 | 0.01 |
| 10:00 LT | 27.71 | 0.02 | 22:00 LT | 28.67 | 0.03 |
| 11:00 LT | 27.69 | 0.01 | 23:00 LT | 28.55 | 0.05 |
| Max | 28.70 (21:00 LT h) | | | | |
| Min | 27.69 (11:00 LT h) | | | | |
| dry season | | | | | |
| Hour | River Temp. (°C) | | Hour | River Temp. (°C) | |
| | Average | Std. Dev. | | Average | Std. Dev. |
| 00:00 LT | 23.90 | 0.02 | 12:00 LT | 23.80 | 0.08 |
| 01:00 LT | 23.88 | 0.02 | 13:00 LT | 23.82 | 0.02 |
| 02:00 LT | 23.80 | 0.06 | 14:00 LT | 23.87 | 0.04 |
| 03:00 LT | 23.74 | 0.04 | 15:00 LT | 23.89 | 0.04 |
| 04:00 LT | 23.71 | 0.04 | 16:00 LT | 24.00 | 0.04 |
| 05:00 LT | 23.66 | 0.01 | 17:00 LT | 23.97 | 0.05 |
| 06:00 LT | 23.64 | 0.01 | 18:00 LT | 23.99 | 0.08 |
| 07:00 LT | 23.60 | 0.04 | 19:00 LT | 24.08 | 0.02 |
| 08:00 LT | 23.57 | 0.03 | 20:00 LT | 24.03 | 0.02 |
| 09:00 LT | 23.59 | 0.01 | 21:00 LT | 24.00 | 0.02 |
| 10:00 LT | 23.62 | 0.02 | 22:00 LT | 23.96 | 0.02 |
| 11:00 LT | 23.65 | 0.02 | 23:00 LT | 23.95 | 0.02 |
| Max | 24.08 (19:00 LT h) | | | | |
| Min | 23.57 (08:00 LT h) | | | | |

Spatial heterogeneity of Chl and CO₂ fluxes

F. S. Pacheco et al.

Title Page

Abstract Introduction

Conclusions References

Tables Figures

◀ ▶

◀ ▶

Back Close

Full Screen / Esc

Printer-friendly Version

Interactive Discussion



Spatial heterogeneity of Chl and CO₂ fluxes

F. S. Pacheco et al.

Table 4. Comparison between CO₂ fluxes (mmol m⁻² d⁻¹) calculated in periods of low retention time and high retention time. Positive fluxes denotes net gas fluxes from the lake to the atmosphere. ^a We considered data for low retention and high retention time when values was less than 25 days and more than 38 days, respectively. The average of the CO₂ fluxes in periods of intermediate retention time was closely to 0 (0.3 mmol m⁻² d⁻¹).

| | CO ₂ fluxes mmol m ⁻² d ⁻¹ | | | |
|----------------------------|---|-----------|---------------------|-----------|
| | Low retention time | | High retention Time | |
| | Average | Std. Dev. | Average | Std. Dev. |
| Temporal data ^a | -17.4 | 23.1 | 10.3 | 27.7 |
| Spatial data | 22.1 | 50.78 | -7.2 | 21.9 |

[Title Page](#)
[Abstract](#)
[Introduction](#)
[Conclusions](#)
[References](#)
[Tables](#)
[Figures](#)
[Back](#)
[Close](#)
[Full Screen / Esc](#)
[Printer-friendly Version](#)
[Interactive Discussion](#)


Spatial heterogeneity
of Chl and CO₂ fluxes

F. S. Pacheco et al.

Title Page

Abstract

Introduction

Conclusions

References

Tables

Figures

◀

▶

◀

▶

Back

Close

Full Screen / Esc

Printer-friendly Version

Interactive Discussion

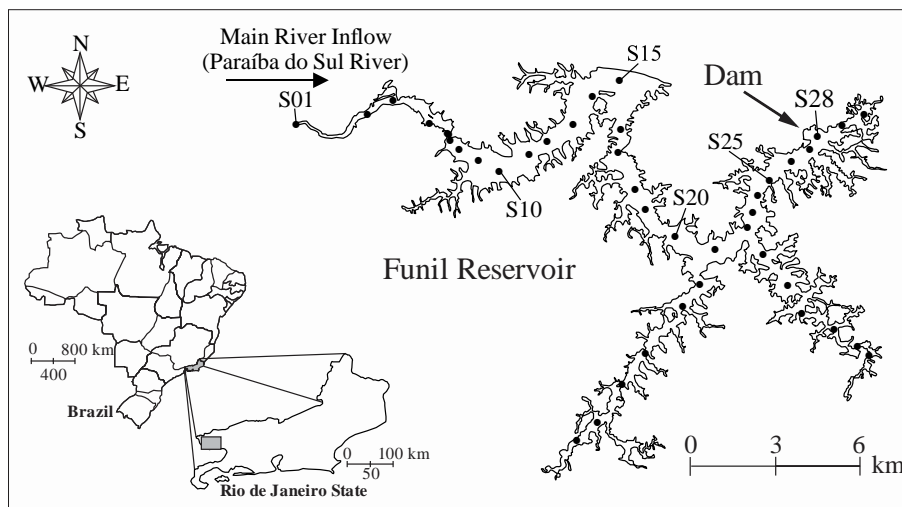


Figure 1. Map of Funil reservoir showing geographic location and sampling stations.

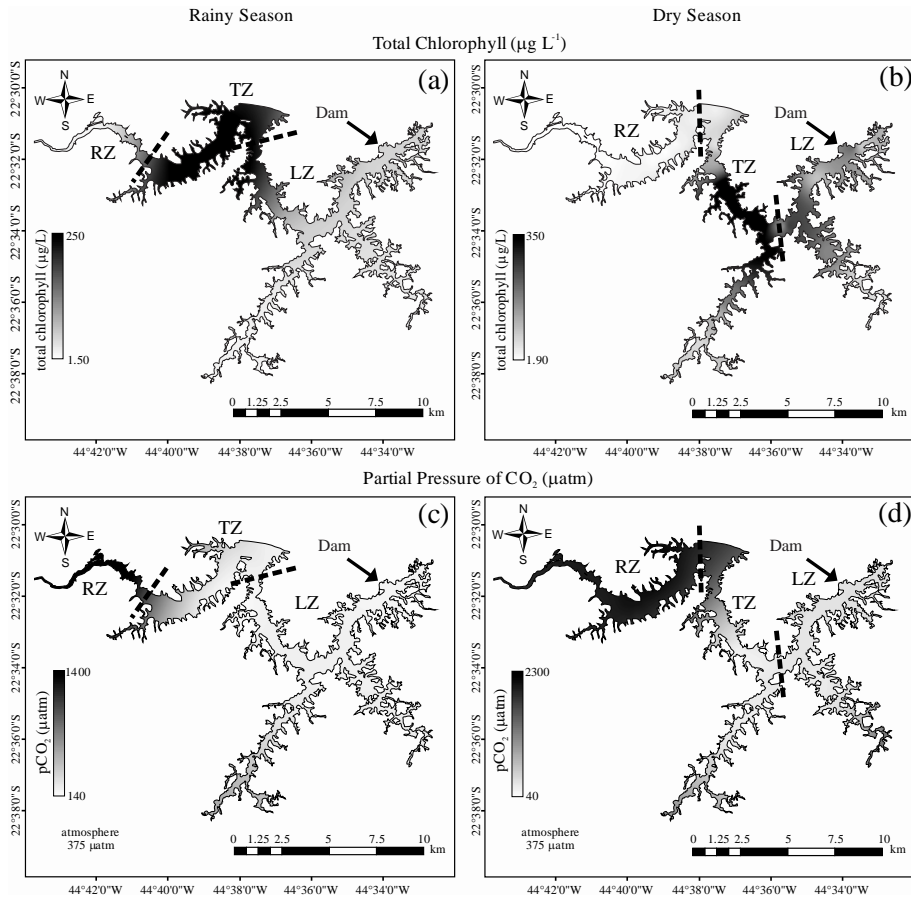


Figure 2. Map of $p\text{CO}_2$ and Chl expressed by a color gradient obtained from interpolation of measured data using the Ordinary Kriging statistical procedures. Lighter gray represent low Chl (a, b) and low $p\text{CO}_2$ (c, d). RZ = Riverine Zone, TZ = Transition Zone, LZ = Lacustrine Zone.

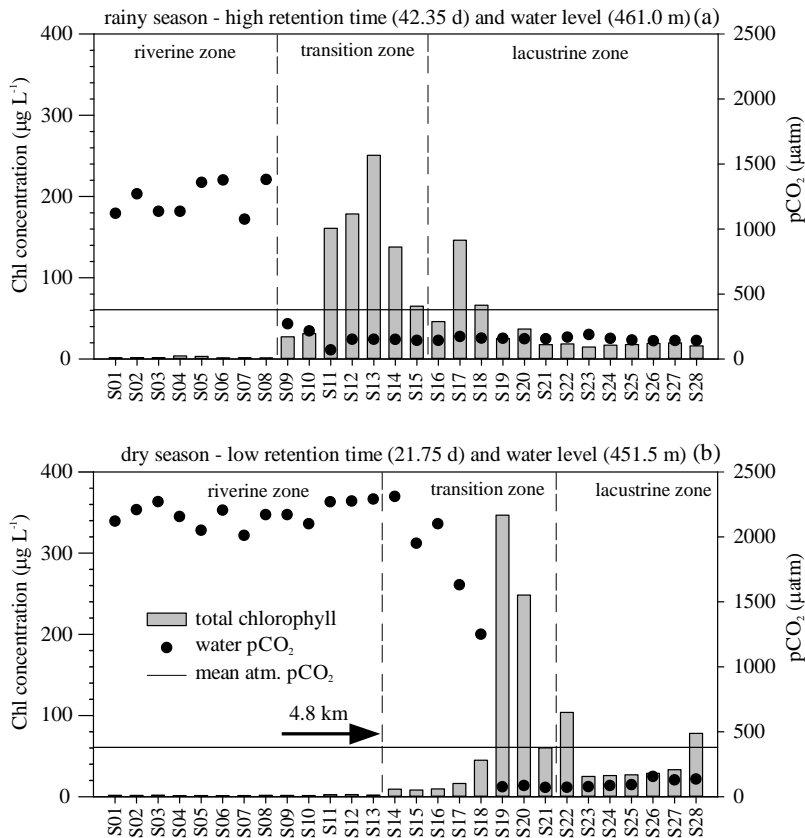


Figure 3. Lotic-lentic gradient of $p\text{CO}_2$ and Chl along the 28 sampling station in the main reservoir body in rainy season (a) and dry season (b). The water level was 461.0 and 451.5 in rainy season and dry season. Three zones can clearly be defined (riverine, transition and lacustrine zone). The arrow shows that the transition zone starts 4.8 km down-reservoir in the period of low water level.

Spatial heterogeneity of Chl and CO₂ fluxes

F. S. Pacheco et al.

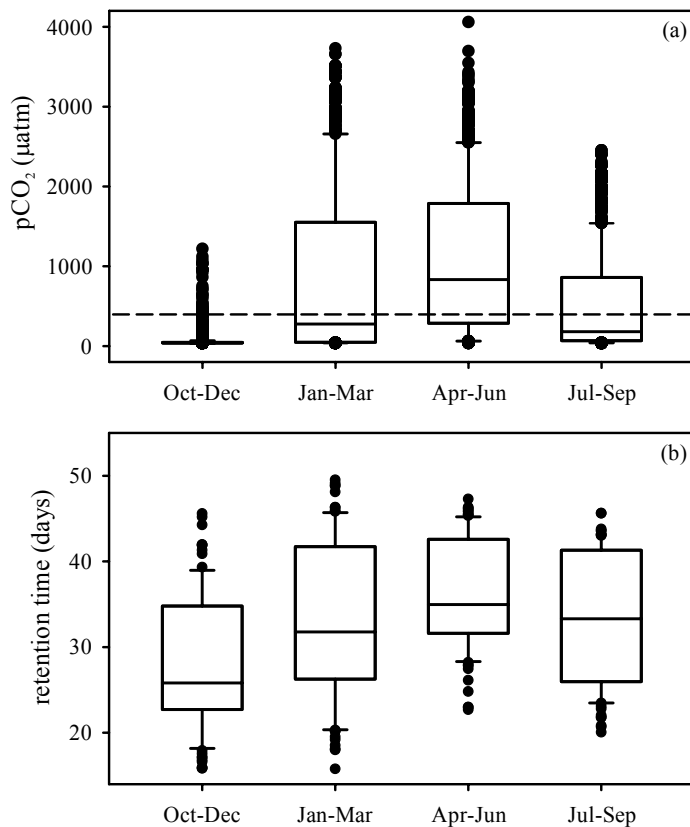


Figure 4. Box plot of $p\text{CO}_2$ at station S28 near the dam **(a)** and mean reservoir retention time **(b)** over the studied year. The dashed line represents the average of $p\text{CO}_2$ in the atmosphere ($375 \mu\text{atm}$). The data are subdivided in four seasons: rainy-spring (October–December), rainy-summer (January–March), dry autumn (April–June) and dry winter (July–September).



Spatial heterogeneity of Chl and CO₂ fluxes

F. S. Pacheco et al.

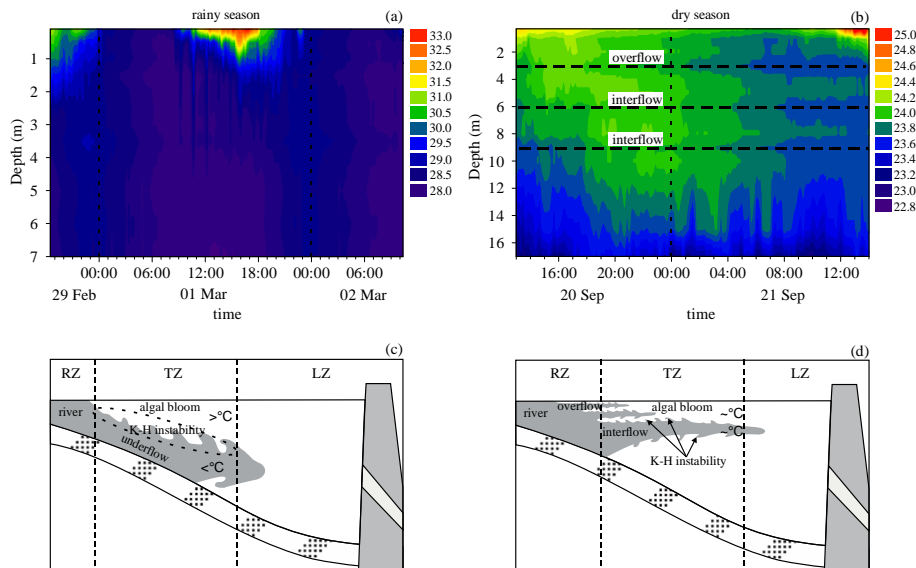


Figure 5. Temperature profile collected at station S09 in rainy season **(a)** and at station S14 in dry season **(b)**. Dashed line represent the depths where river flows as overflow or interflows. In rainy season the river plunges and flows under the reservoir (underflow) due to difference of density **(c)**. Waves and billows develops along the interface due to shear velocity (Kelvin–Helmholtz instability) and facilitate vertical mixing (see text). In dry season the river flows as overflow or interflow **(d)** since the difference of density between river and reservoir is low. At this situation, the river can influence the reservoir surface water more 5 kilometers toward the dam. RZ = Riverine Zone, TZ = Transition Zone, LZ = Lacustrine Zone.

Spatial heterogeneity of Chl and CO₂ fluxes

F. S. Pacheco et al.

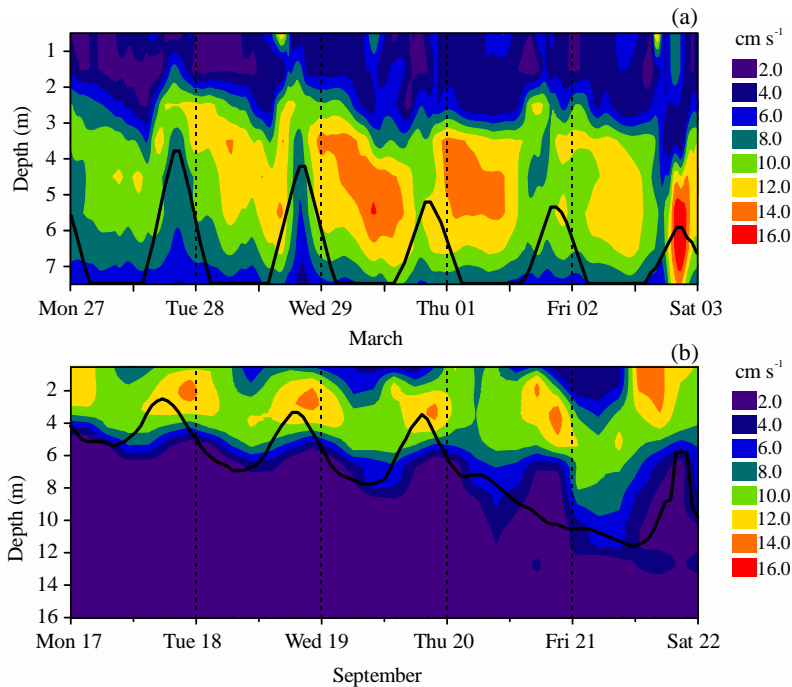


Figure 6. Simulated velocity profile using realistic forcing. Higher velocities represent the depth where the river flows through the transition zone. The river flows as underflow in rainy season when a denser (colder) river plunges beneath the surface and it will flow downward along the bottom as a gravity-driven density current **(a)**. The river flows as overflow in dry season when temperature from river and reservoir are similar. **(b)** As overflow, the river characteristics can be found many kilometers toward the dam at surface water. The black line represents the depth of neutral buoyancy estimated from temperature records, presuming that lake and river water do not mix. The anomaly observed in the river flow and depth of neutral buoyancy between 20 and 21 September 2012 occurred due to a decrease of the river temperature during a rainfall that occurred around 16:00 LT on 20 September.

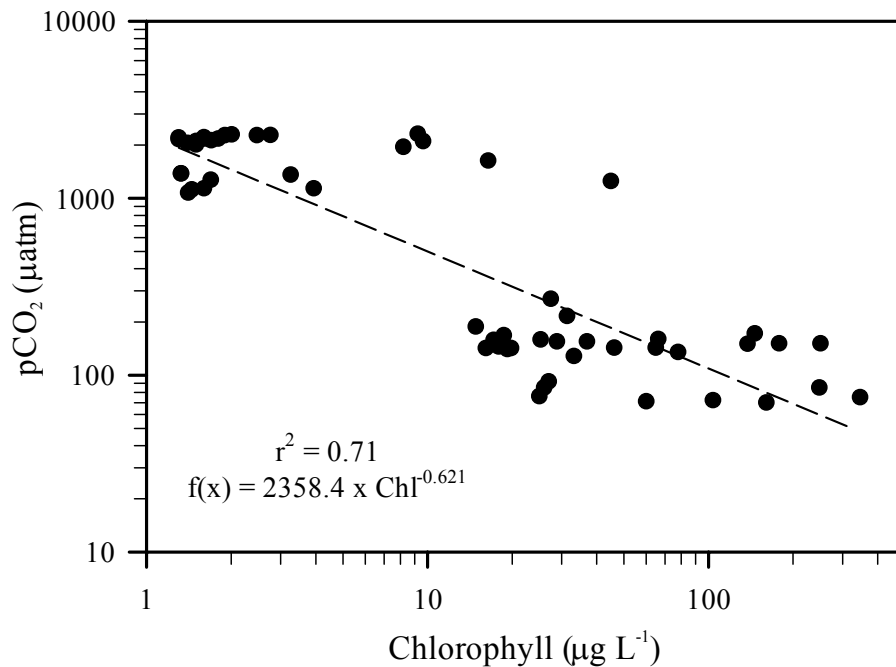


Figure 7. Relationship between spatial data of $p\text{CO}_2$ and Chl in Funil Reservoir. The regression is represented by dashed line ($r^2 = 0.71$, $p < 0.001$).

Spatial heterogeneity of Chl and CO_2 fluxes

F. S. Pacheco et al.

[Title Page](#)

[Abstract](#) | [Introduction](#)

[Conclusions](#) | [References](#)

[Tables](#) | [Figures](#)

[◀](#) | [▶](#)

[◀](#) | [▶](#)

[Back](#) | [Close](#)

[Full Screen / Esc](#)

[Printer-friendly Version](#)

[Interactive Discussion](#)

